Available online at www.sciencedirect.com

ScienceDirect

Procedia Structural Integrity 52 (2024) 28–42

Structural Integrity Procedia

www.elsevier.com/locate/procedia

Fracture, Damage and Structural Health Monitoring

Critical Analysis of MP-TP Wedge Connection Concept for Application in Offshore Wind Turbines

Alessandro Annoni[a] and Ali Mehmanparast[a]*

[a] *Department of Naval Architecture, Ocean and Marine Engineering, University of Strathclyde, Glasgow G1 1XQ, United Kingdom*

Abstract

The main technologies that have been employed in the offshore wind industry for connecting the monopile foundation to the transition piece (MP-TP) are the grouted connection and threaded connection. The latter has been widely used in the majority of offshore wind farms developed in the last decade. However, as the offshore wind turbines get larger in size to increase the level of produced electricity, there is an essential need to re-evaluate the use of threaded joints as the current main choice for MP-TP connections and develop new MP-TP concepts which offer lower costs. An innovative MP-TP technology which has been developed for application in offshore wind industry is the wedge connection concept. In this paper, an independent study has been conducted through analytical evaluation and finite element analysis to understand the technological benefits that this concept offers. The study has been developed in three different steps: design of hole geometry, stress distribution prediction and a real-case scenario to evaluate the strength of the system under different loading conditions. The results from this study have been discussed in terms of the main advantages that the wedge connection technology offers as an alternative MP-TP concept for offshore wind applications.

Keywords: Offshore wind turbine; MP-TP connection; wedge connection; structural design

* Corresponding author.
E-mail address: ali.mehmanparast@strath.ac.uk

10.1016/j.prostr.2023.12.004

1. Introduction

Offshore wind is an efficient and reliable source of renewable energy which is exponentially expanding around the world, particularly in Europe. Offshore Wind Turbines (OWTs) consist of three general parts which are namely foundation, tower and the transition piece (TP) in between. The dominant type of foundation which is successfully employed in many of the offshore wind farms around the work to support OWTs is monopile (MP) (1,2). One of the important engineering challenges associated with the design and operation of OWTs is the connection technology between the monopile and the transition piece (MP-TP). In the past three decades the MP-TP concepts that have been widely utilised in offshore wind farms are grouted and flange bolted connections. The grouted connection has been historically used for many years in the offshore Oil & Gas industry and was the first technology employed for offshore wind turbine MP-TP connection. Using this technology, the transition piece is set on the monopile and plugged on it by aligning the two axes and the gap between the two cylinders is subsequently filled in with grout. Despite the advantages that the well-known grouted connection technology offers, in the 2010s a number of fatigue failures were observed in commissioned OWTs which obligated the offshore wind industry to consider alternative technologies for MP-TP connection in the following offshore wind projects.

As a result of this, the industry heavily moved towards flange bolted connection (also known as threaded connection). Using this technology, L-flanges are welded to the bottom of the transition piece and top of the monopile and are kept together with large-scale bolts and nuts which are equally spaced around the circumference of the MP-TP geometry. This technology provides a series of benefits such as a direct load path with the possibility to have easy access for inspection and monitoring. However, the threaded connection is affected by environmental and operational loading conditions and pre-load relaxation and fatigue cracks may occur in the bolt and nut connection which would affect the structural integrity of the OWTs (3–5)

According to the European reports (6), the offshore wind installed capacity in Europe is continuously increasing and the turbine dimensions are growing accordingly. This means that for larger wind turbines, there will be need for larger and stronger foundations. Therefore, it becomes necessary to re-evaluate the use of threaded technology and consider alternative technologies for MP-TP connections in future OWTs. One of the new and promising MP-TP concepts that has been proposed in recent years to overcome the current issues faced by industry is the C1 wedge connection. This technology consists of redesign of the L-flanges by converting the vertical connection into a horizontal one through the design of a cylindrical lower flange for the MP section with a fork-shaped upper flange for the TP section. According to this concept, a series of elongated holes will be accommodated around the circumference of the geometry allowing the positioning of the C1 wedge fastener which are pushed in using horizontal bolts and would hold the two flanges together by creating a preload.
The aim of the present study is to conduct an analytical evaluation and finite element analysis (FEA) to understand the technological benefits of the C1 wedge connection concept. In order to achieve this goal, the following objectives have been defined and thoroughly investigated: i) to design the hole geometry, ii) to predict the stress-distribution around the hole geometry, and iii) to evaluate the strength under different loading conditions in a real-case scenario.

2. Hole geometry

Considering a simplified layout of the monopile geometry (see Figure 1), its external circumference C can be calculated according to the following equation:

$$C = \pi D_{tower} = nl + nD_{hole} = nW \quad (1)$$

where n is the number of holes along the circumference, D_{hole} is the hole diameter, D_{tower} is the external tower diameter, $\boldsymbol{l}$ is the ligament width between the holes.

Moreover, the following equations would describe the correlation between different parameters such that:

$$l = \frac{\pi D_{tower} - nD_{hole}}{n} \tag{2}$$

$$\frac{l}{D_{hole}} = \frac{\pi D_{tower} - nD_{hole}}{nD_{hole}} = \frac{H - D_{hole}}{D_{hole}} \tag{3}$$

where H is the tower equal section, and *W* is the tower's width segment. In this paper, the *l/D* hole ratio will be considered to have an equal proportion in the analysis.

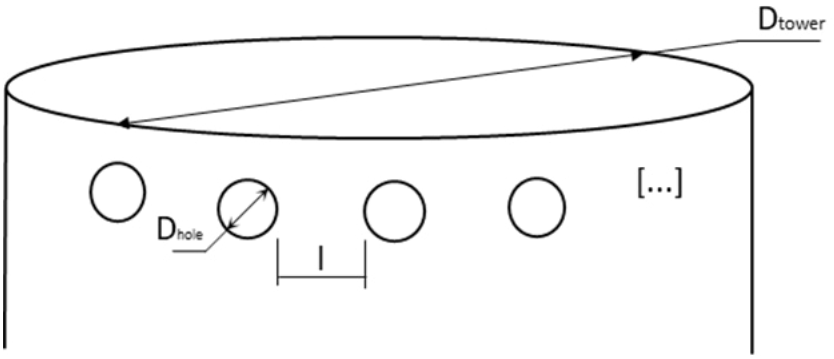

Figure 1: Simplified MP geometry for wedge connection

Treating the MP-TP wedge connection as a series of segments of width *W,* it is possible to consider each segment as a pin-loaded lug, giving the possibility of tackling the problem as the contact between two cylinders of equal length with parallel axes.

The Hertz model has been commonly used to calculate the contact stress in engineering calculations (7). This mathematical method is based on three assumptions: 1- the surfaces are smooth and frictionless, 2- the contact area is small compared to the size of the bodies, and 3- the bodies are under little deformation and in the state of full elasticity.

According to the Hertz model, the total contact length, 2*b*, between pin and lug can be calculated using:

$$2b = 2\sqrt{\frac{2F}{\pi t}\frac{(1-\varepsilon_1{}^2)/E_1 + (1-\varepsilon_2{}^2)/E_2}{1/D_1 + 1/D_2}} \tag{4}$$

where *F* is the total applied load, *t* is the cylinder length, D_i is the diameter for the pin (D_1) and the hole (D_2), and ε_i and E_i are the Poisson's Ratio and Young's modulus for the pin and lug material.

To calculate the contact angle $2\alpha_i$ the following equation can be used:

$$2\alpha_i = 2a \times \sin\left(\frac{2b}{D_i}\right) \tag{5}$$

The maximum pressure can be calculated as:

$$p_{max} = \frac{2F}{\pi bt} \tag{6}$$

Finally, the stresses along the x, y and z directions can be described using the following equations:

$$\sigma_x = -2\varepsilon p_{\max}\left(\sqrt{1+\frac{z^2}{b^2}} - \left|\frac{z}{b}\right|\right) \tag{7}$$

$$\sigma_y = -p_{\max}\left(\frac{1+\frac{2z^2}{b^2}}{\sqrt{1+\frac{z^2}{b^2}}} - 2\left|\frac{z}{b}\right|\right) \tag{8}$$

$$\sigma_z = -\frac{p_{\max}}{\sqrt{1+z^2/b^2}} \tag{9}$$

As mentioned previously, the Hertz model requires a frictionless contact surface; however, as illustrated in (8) it is possible to create an updated model to take in consideration the friction coefficient. In a real life scenario, the friction coefficient is a non-zero value, for instance in the case of steel on steel contact without lubrification or finish processing the friction coefficient can be taken as μ=0.15. Having said that, the frictionless assumption provides simplified solutions for engineering problems.

In the present study, the hole geometry has been studied by considering a stadium shaped geometry. Through FEA simulations, the stadium shaped geometry has been redesigned and optimised using a double radius technique which is illustrated in Figure 2. For the optimization of the shape two groups of FEA simulations have been run, the first group to understand how the stress concentration factor (SCF) changes in accordance with the slope of the tangential edge of the two radius *Φ*, and the second group to understand how the SCF is affected by the plastic proprieties of the material.

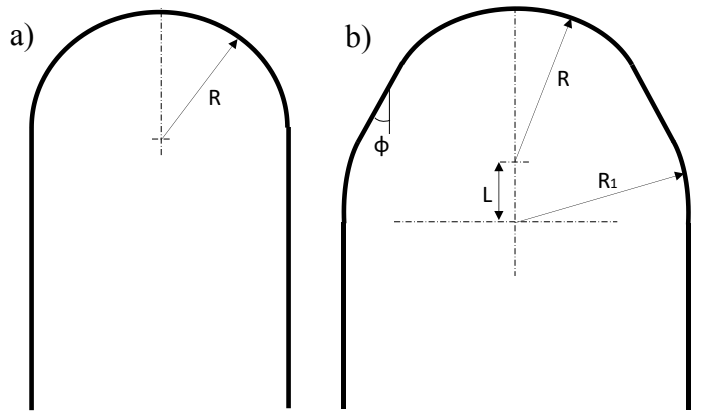

Figure 2: Differences between stadium shape (a) and double radius shape (b) geometry

3. Fastener

The C1 wedge connection fastener is comprised of two blocks (upper and lower), 2 wedges (inner and outer) and a lateral bolt. The design of the fastener allows a high preload being applied through relatively easy and low load tightening of the lateral bolt. By torquing the lateral bolt, the two wedges will be pushed toward each other and this mechanism would pull the upper and lower blocks away from each other. This movement will introduce a preload in the connection which would subsequently create a contact between the MP and TP. To understand the C1 wedge connection technology design two main studies have been developed in this study: the optimization of the hole shape and the fastener's performance. There are two factors that are analysed in the present study for understanding of the wedge connection performance: 1- the load performance LF (Load Factor), and 2- displacement performance DF

(Displacement performance). Both of these factors show the correlation between the vertical and horizontal components of load and displacement.

To calculate the preload force on the bolt (F_{bolt}) a Free Body Diagram (see Figure 3) to describe the forces as follows:

$$\sum F_{Hor} = 0 \tag{10}$$

$$F_{bolt} = F_{hor_1} + F_{hor_2} + F_{friction_{1_{hor}}} + F_{friction_{2_{hor}}} \tag{11}$$

$$F_{hor_i} = \frac{F_P}{2}\tan(\theta) \tag{12}$$

$$F_{friction_i} = \frac{F_P}{2}\cos(\theta)\,\mu_i \tag{13}$$

$$F_{frict_{i_{hor}}} = F_{frict_i}\cos(\theta) \tag{14}$$

where the subscript i is referring to the upper block as 1 and the lower one as 2, and θ is corresponds to α and β for the wedge slope of the upper and lower blocks, respectively.

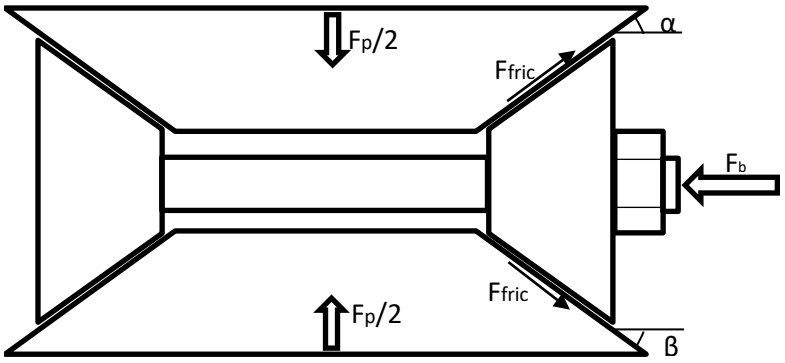

Figure 3: Free Body Diagram for C1 wedge connection

Considering a value of α for the upper wedge slope and β for the lower wedge slope, the Equation 11 can be rewritten as:

$$F_{bolt} = \frac{F_P}{2}[\tan(\alpha) + \tan(\beta)] + \frac{F_P}{2}\mu[\cos^2(\alpha) + \cos^2(\beta)] \tag{15}$$

From Equation 15, it can be observed how the system is affected by the wedge angle inclination of the upper and lower block and from the friction coefficient between the blocks and the wedge.

In Equation 16 the Load Factor, LF, has been described as:

$$LF = \frac{F_P}{F_{bolt}} = \frac{2}{[\tan(\alpha) + \tan(\beta)]} + \frac{2}{\mu[\cos^2(\alpha) + \cos^2(\beta)]} \tag{16}$$

As illustrated in Figure 4, the total vertical displacement ($\Delta d_{vertical}$) can be calculated as:

$$\Delta d_{vertical} = \Delta d_{horizontal}[\tan(\alpha) + \tan(\beta)] \tag{17}$$

In Equation 18 the Displacement Factor has been calculated

$$DF = \frac{\Delta \mathrm{d}_{\mathrm{vertical}}}{\Delta \mathrm{d}_{\mathrm{horizontal}}} = \tan(\alpha) + \tan(\beta) \tag{18}$$

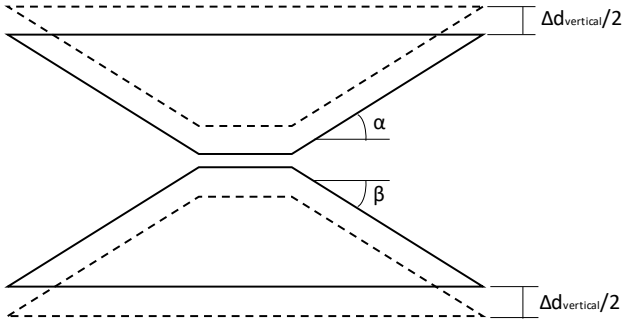

Figure 4: Total vertical displacement

4. Results

4.1. Hole shape geometry

The Hertz model was used to develop an optimised hole shape by taking into consideration the contact angle. For this purpose Equation 5 has been plotted in Figure 5 considering the input data in Table 1.

Table 1: Hertz model data

Input data	
D_{hole} [mm]	100
t [mm]	80
E_{hole} [GPa]	210
E_{pin} [GPa]	210
Poisson's ratio wall (ε_{wall})	0.3
Poisson's ratio pin (ε_{pin})	0.3
Applied load [N]	2.3×10^6

As seen in Figure 5, a prediction of the angle of contact (2α) as a function of the ratio between the pin diameter and the hole diameter has been calculated. The curves are generated based on frictionless surface contact, so it is known that the predicted values are only estimates and may not be 100% accurate for a real case scenario with non-zero friction coefficient value.

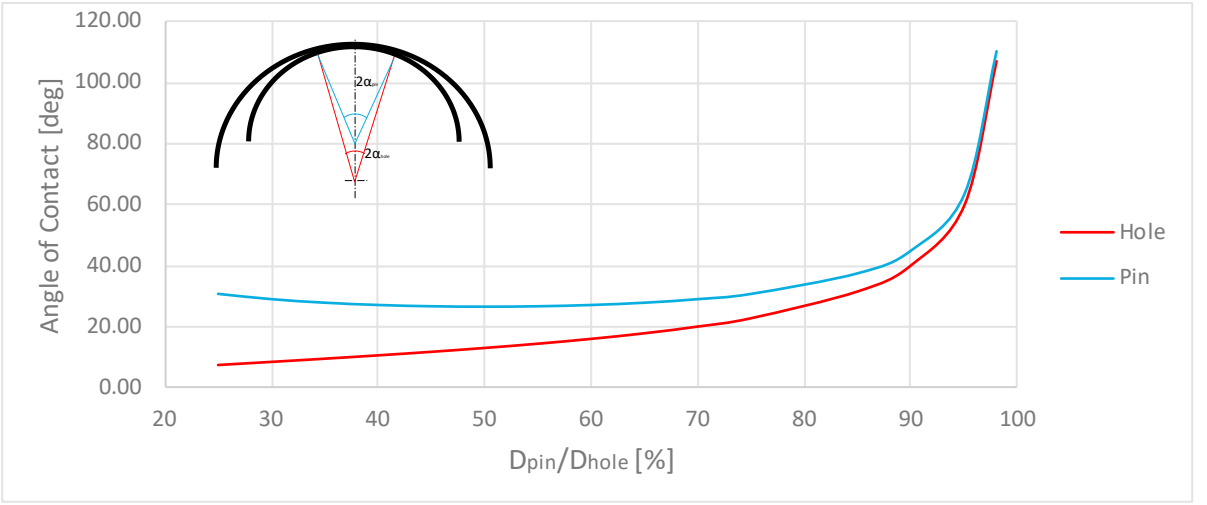

Figure 5: Hertz model angle contact

In the next step, the stress distribution along the y and z directions are considered to decide which of the *Dpin/Dhole* ratio to use. Equation 8 and 9 have been plotted in Figure 6 and the generated curves show how higher stresses are obtained for smaller diameter ratio while for ratio close to 1 the stress is smaller due to the higher contact surface, under the same load condition. From this preliminary consideration, a Dpin/Dhole ratio of 0.99 is selected and will be considered for the next phase of the analysis.

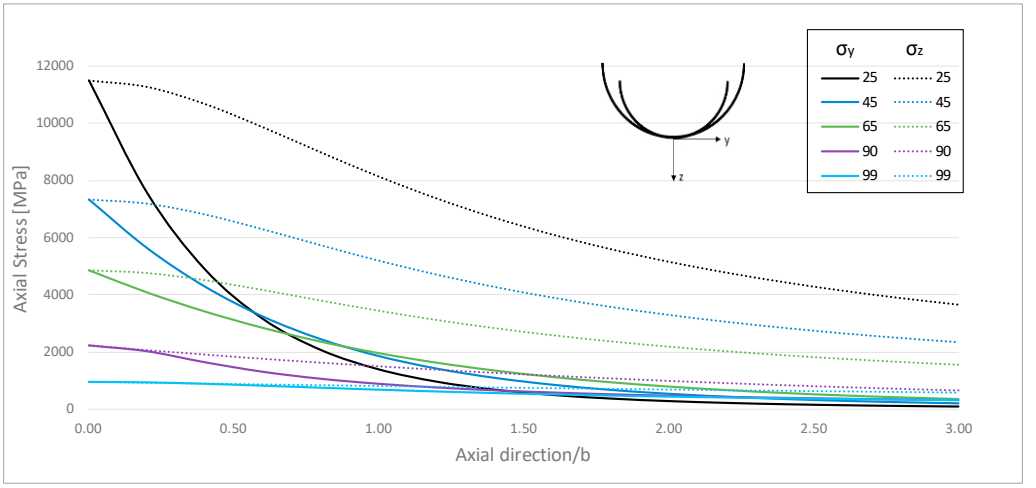

Figure 6: Stress profile along Y (solid) and Z (round dot) axis for different Dpin/Dhole ratio: 0.25 (black), 0.45 (blue), 0.65 (light green), 0.9 (purple) and 0.99 (azure)

The aim of the optimisation of the hole shape is to be able to move the maximum stress as far away as possible from the contact area. For this analysis a series of FEA models have been studied and the main dimensions have been reported in Table 2 and Table 3. The dimensions have been scaled considering a l/D ratio of 1.9 considering D as the diameter of larger radius ($2R_1$).

Table 2: FE Analysis variable dimensions

Simulation	1	2	3	4	5
W [mm]	159.5	174	166.75	159.5	174
R_1 [mm]	55	57.5	60	55	57.5
L [mm]	10	10	10	20	20

Table 3 FE Analysis constant dimension

R [mm]	50
H [mm]	250
c [mm]	50
t [mm]	40
E_{hole} [GPa]	210
E_{pin} [GPa]	220
Poisson's ratio wall (ε_{wall})	0.3
Poisson's ratio pin (ε_{pin})	0.3

The results obtained from the purely elastic analysis have been reported in Figure 7. The two main factors reported are the SCF and the angular position, θ, of the maximum stress point from the centre of the D_1 circle. The explanation of this factor is as follows:

- The SCF have been used as qualitative value, considering that the pure elastic behaviour in the FEA simulation will not be taken as the final result but for the design optimisation of the hole the smallest possible value will be found.
- Φ can be read as how far the maximum stress value is positioned compared to the contact area. A Φ value of close to 90 [deg] means that the maximum stress point is exactly on the maximum Hertz contact pressure point and a Φ value of close to 0 [deg] means that the maximum stress is at the beginning of the R1 radius. For the optimisation purpose, a low Φ angle will be considered.

Based on the explanations provided above and the obtained results, the optimum model is the one from simulation number 3, hence this model is considered for further analysis by employing plastic properties in the simulation.

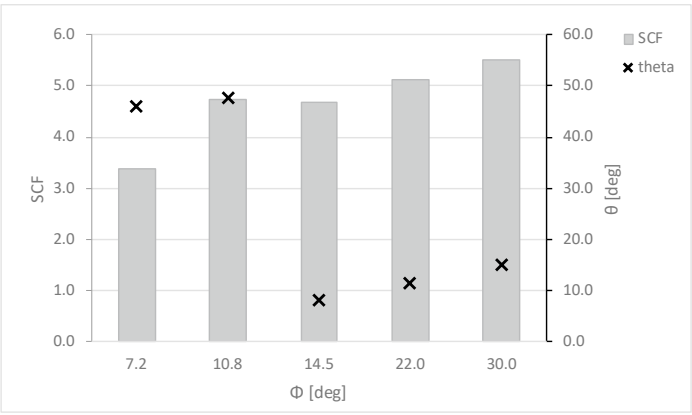

Figure 7: Stress profile: SCF (column) and angular position (square) for pure-elastic FEA analysis

4.2. Fastener

Equations 16 and 18 have been plotted in Figure 8 and Figure 9, respectively as function of α and β angles and considering a friction coefficient of 0.05. As seen in these figures the Load Factor is lower than 1, which means that the horizontal load is higher than the vertical load but for lower angle values the Load Factor increases to up to 20 for a double flat wedge connection. From Figure 9 it can be seen how the Displacement Factor changes as a function of the wedge inclinations. Comparing the results to the Load Factor trend it can be seen how the Displacement Factor shows opposite behaviour and for a higher slope a greater vertical displacement is achieved whereas for lower inclination angle the value is lower up to 0 for α and β of equal 0 [deg]. This means that, to provide a minimum displacement, at least one of the wedge angles need to be higher than 0 [deg].

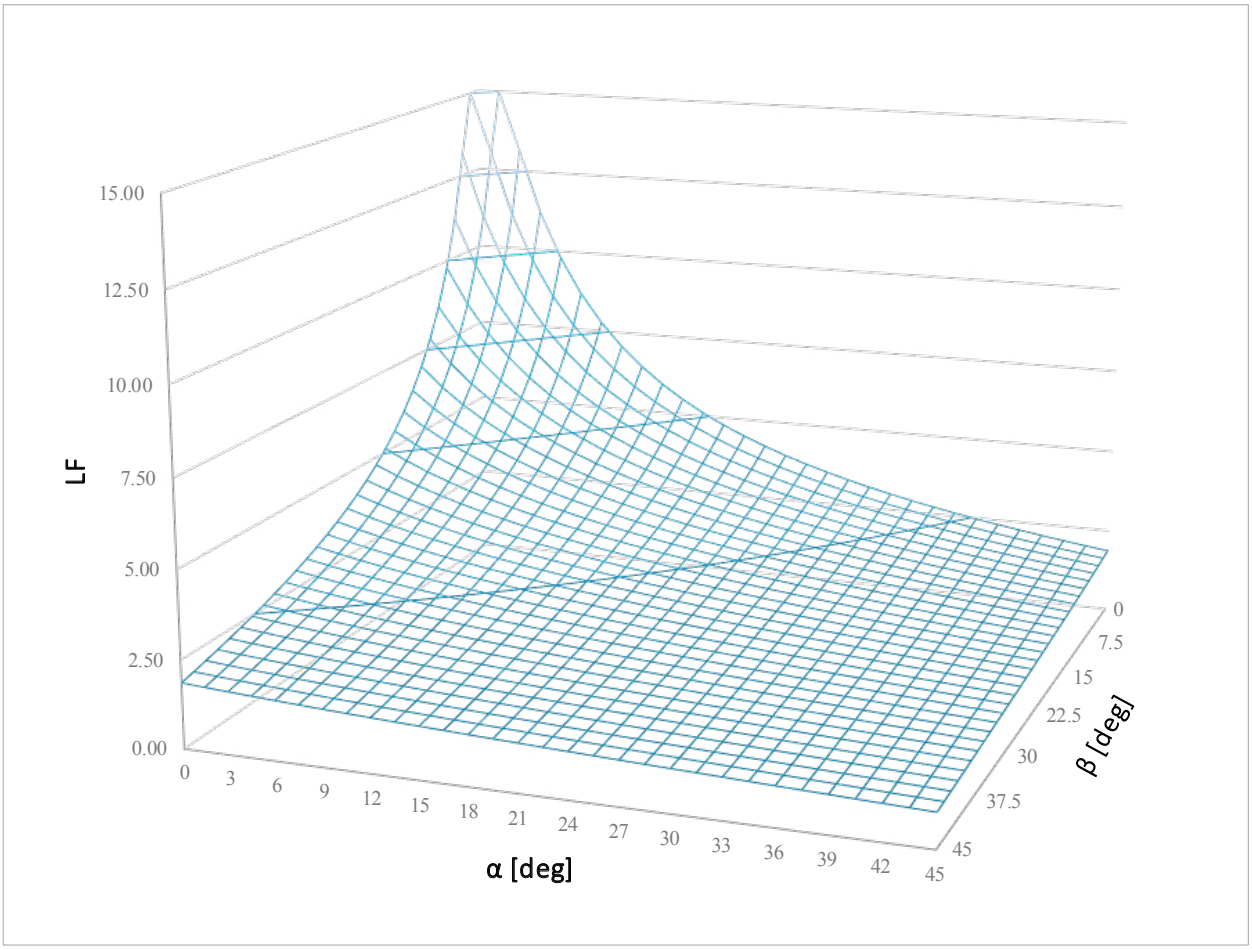

Figure 8: Load Factor (LF) variation against alfa and beta

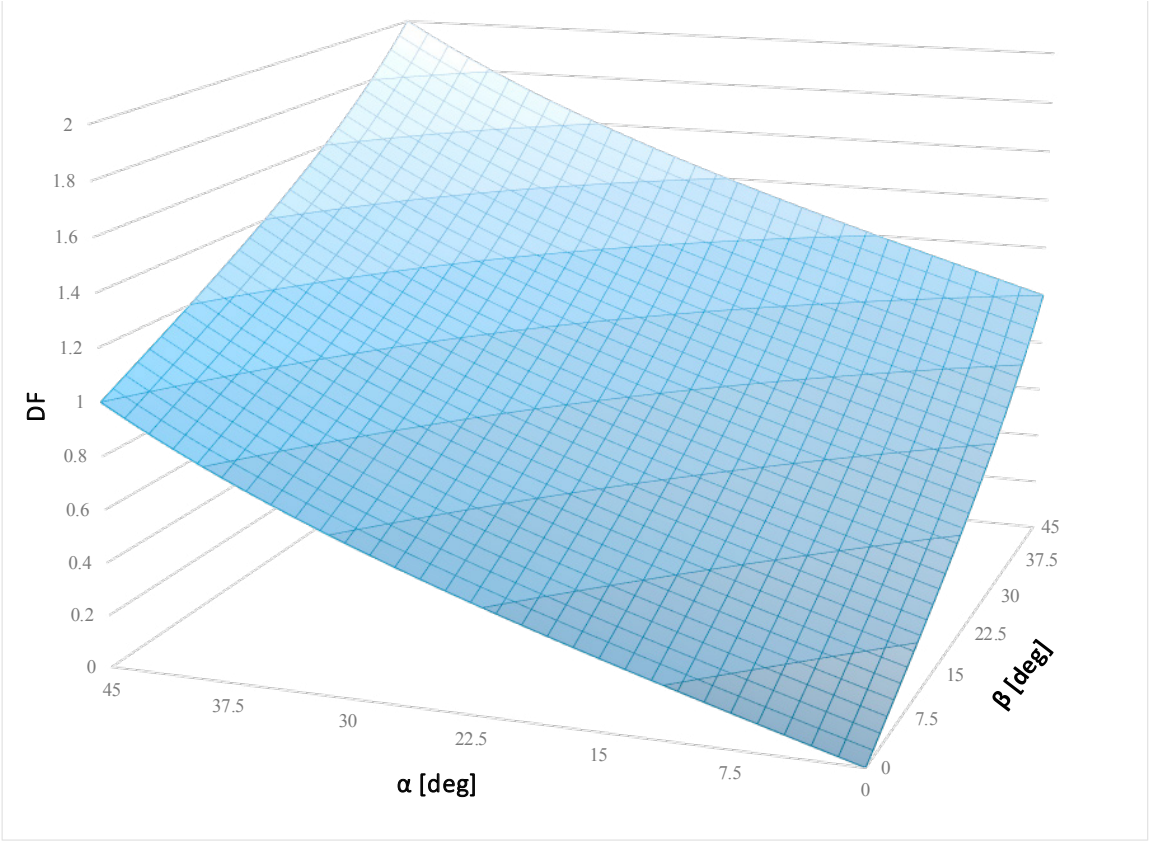

Figure 9: Displacement Factor (DF) variation against alfa and beta

In Figure 10, two different wedge inclination layouts have been considered in order to see how the LF changes with different friction coefficient values. As seen in this figure, the LF increases with a reduction in the friction coefficient, for this reason it is necessary to have the lowest value between the wedge components and the blocks.

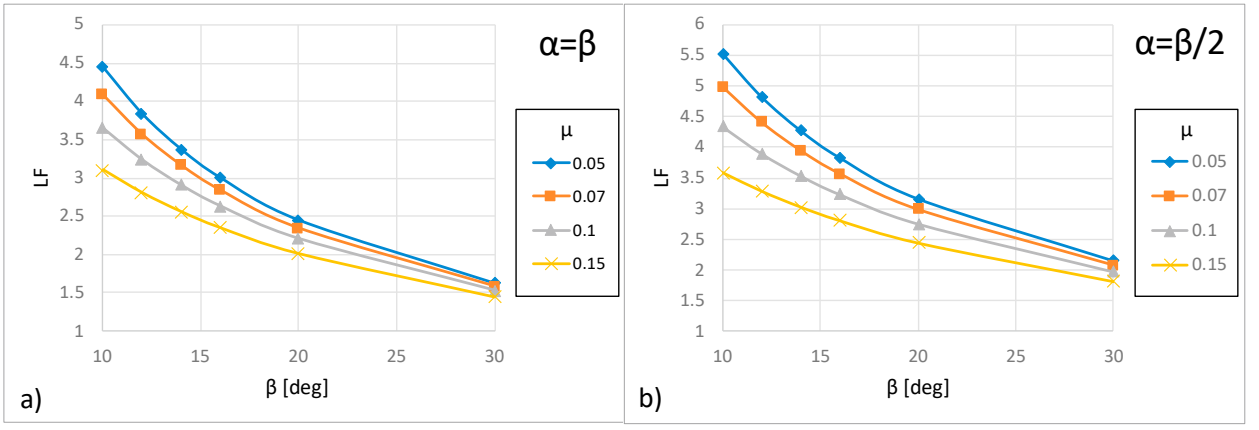

Figure 10: LF variation with different friction coefficient factor for different slope wedge inclination: a) α=β and b) α=0.5β. Friction coefficient factors: 0.05 (blue), 0.07 (red), 0.1 (green) and 0.15 (purple)

4.3. FEA Analysis

Under the global loading condition, an MP-TP wedge connection was modelled and studied by means of FEA simulation. For the purpose of this case study, a general 6 MW offshore wind turbine with the dimensions reported in Table 4 were employed (9,10). A Vertical Load of 2.3 MN has been used, taking under consideration the overall bending effect and applied on a single section of the tower.

Table 4: Offshore wind turbine dimensions

	Dimension
Blade radius [m]	75
Distance of nacelle from water level [m]	80
Diameter of tower [m]	6
Wall thickness of tower (t) [mm]	80

The simulation takes into consideration all of the previous observations showed previously in the study and considers an elastic-plastic model to describe the material behaviour. The main dimensions of the connection have been reported in Table 5 and the friction coefficients considered are reported in Table 6. In Table 5, R is the main hole radius of the contact area between the block and the hole, R_1 is the secondary radius, R_{block} is the block radius (R_{pin} showed previously), θ is the inclination of the , α and β are the slope angle of the upper and lower block , t_MP and t_{TP} are the wall thickness of Mono-Pile and Transition-piece respectfully.

Table 5: FEA model dimensions and material proprieties

	Dimension
R [mm]	50.5
R_1 [mm]	55
R_{block} [mm]	50
θ [deg]	20
α, β [deg]	8
t_{MP} [mm]	80
t_{TP} [mm]	40

Table 6: Friction coefficients employed in the FEA model

Contact surface	Value
Block-Wedge	0.06
MP-TP	0.1
Wedge-Wall	0.1

The materials considered in the analysis as follows:

- S460N steel for the Monopile and the Transition Piece, with the Young's module of 210 [GPa] and the stress-strain curves for different thickness values shown in Figure 11
- 34CrNiMo6 steel for the fastener component with the Young's module of 210 [GPa]

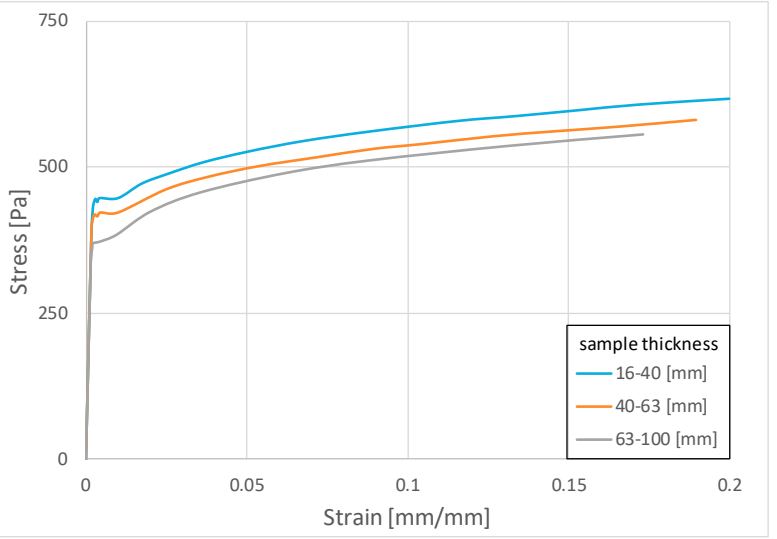

Figure 11: S460N Stress-Strain curves

The load application in the simulation was applied in two steps: a preload phase and the 2.3MN load application. The first phase is necessary to avoid any movement of the connection which could cause a premature failure of the entire structure, for this reason a 2.4 [MN] preload (F_P) was applied. The second phase was the application of 2.3[MN] load on the top of the fork shape section (TP). The load application timeline defined in various simulation steps can be seen in Figure 12.

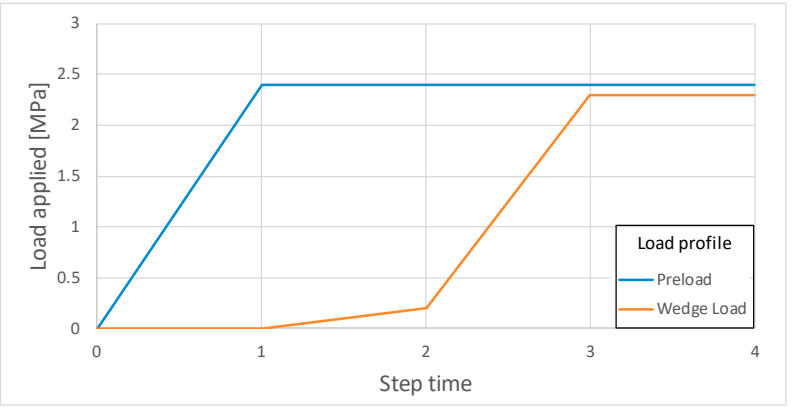

Figure 12: FEA Load application in different steps: Vertical preload (orange) and Vertical load (orange)

Three main results from FEA simulations have been considered: stress distribution in both load steps, the axial stresses and contact angle comparisons with the results obtained from the Hertz model. The stress distribution has been studied for the two flanges separately, each one in preload and load step. As illustrated in Figure 13, can be seen that the high stress region (red region) has a von-Mises stress value close to the yield stress by considering different thicknesses (80 [mm] for MP and 40 [mm] for each web leg of the TP) in the FEA model.

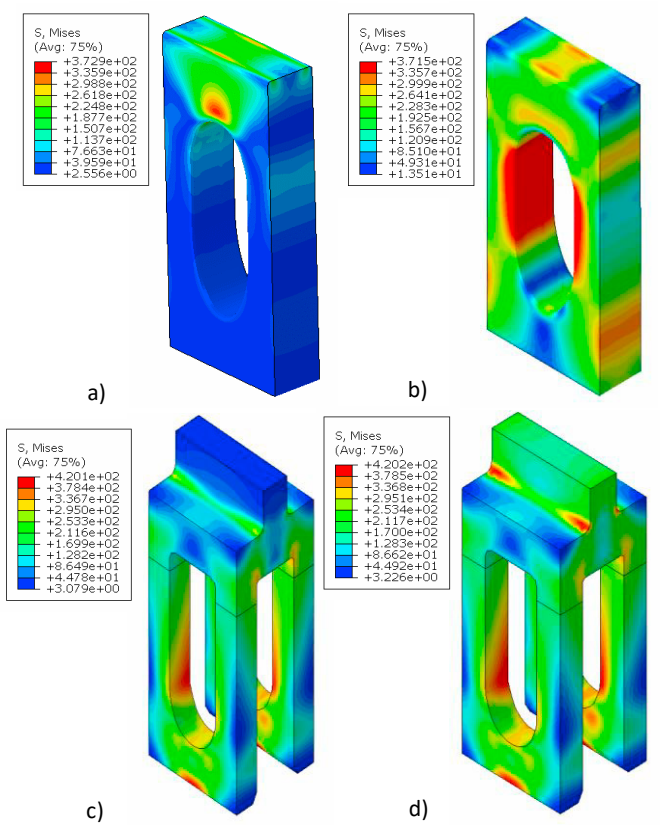

Figure 13: FEA results in preload step for MP (a) and TP (c) and external load step for MP (b) and TP (d)

The FEA results have been compared with the Hertz model focusing on the axial stress distribution along the y and z axis and the contact angle. As seen Figure 14, the results from FE analysis are lower than the mathematical model estimation. This can be linked to the assumptions under which the Hertz model has been developed (frictionless and elastic behaviour) and the interaction between the fastener components that can absorb part of the stress. Similar consideration can be taken from the contact angle which is 18% lower than the(4) expected value (88 [deg]).

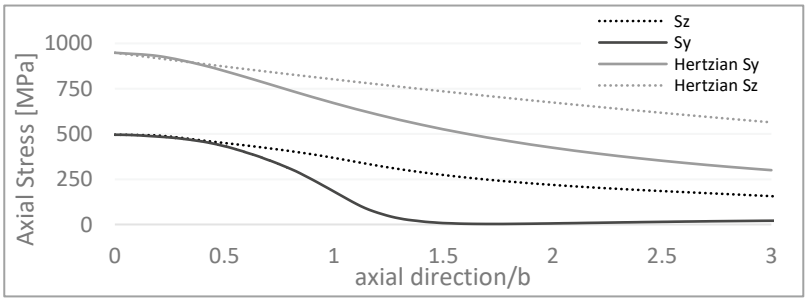

Figure 14: Axial Stress FEA results (black) compared to Hertz model (grey)

To evaluate this technology, a comparison with bolted connection would be necessary by considering load requirements and approximate mass of the fastener. According to Equation 16, with a symmetric slope between the upper and lower wedge of 8 [deg], the LF is equal to 5.28. This means that to apply a 2.4 [MN] of vertical preload a much lower load needs to be applied on the horizontal bolt (~430 [kN]), which agrees with analytically studies (11). In offshore wind industry the typical preload applied on the bolts is equal to or less than 90% of the material's yield stress (and the upper safely limit), which for a M72 bolt is approximately 2.9 [MN] as axial load.

Regarding the load requirements for the fastener another consideration need to be taken which is the mass. C1 wedge connection (considering the bolt, the blocks and the wedges) has a mass of around 15[kg] whereas the bolted connection (considering a M72 bolt, the washer and a nut(12)) has a mass around of between 15 and 19 [kg]. Considering the entire MP-TP connection the number of fasteners required increase drastically with an increase in the diameter. For example, for C1 wedge connection a *l/D* ratio of 2.02(11,13) on a 7 [m] tower diameter results in around 110 fasteners for a total mass of 1650 [kg]. For the bolted connection, according to the EN 1990-1(14), a pitch distance of 2.5 times the bolt diameter need to be considered, so for the same diameter 122 fasteners are required, taking a total mass to the system of 1830-2318 [kg]. These considerations have been taken only on the preliminary FEA analysis and without any optimisation of the C1 wedge connection which can reduce the volume of the fastener, and which would reduce the mass accordingly.

Conclusions

To meet the increasing demand of energy around the world the offshore wind industry needs to increase the dimensions of the future wind turbines. This increases the load applied on the structure and introduces significant challenge for the current MP-TP connections technologies. For this reason, new technologies must be developed, such as C1 wedge connection, to provide safer and more reliable connections. The results presented in this paper demonstrate that the C1 wedge technology requires a detailed engineering and optimising process considering the friction coefficient between the different surfaces, the fastener geometry and the hole shape. However, as results show the load magnitude in the assembling phase is lower compared to the bolted connection and the structure shows a high stress hence fatigue resistance.

References

1. Mehmanparast A, Brennan F, Tavares I. Fatigue crack growth rates for offshore wind monopile weldments in air and seawater: SLIC inter-laboratory test results. Mater Des. 2017 Jan 15;114:494–504.
2. Mehmanparast A, Taylor J, Brennan F, Tavares I. Experimental investigation of mechanical and fracture properties of offshore wind monopile weldments: SLIC interlaboratory test results. Fatigue Fract Eng Mater Struct [Internet]. 2018 Dec 1 [cited 2023 Mar 29];41(12):2485–501. Available from: https://pureportal.strath.ac.uk/en/publications/experimental-investigation-of-mechanical-and-fracture-properties-/fingerprints/
3. Mehmanparast A, Lotfian S, Vipin SP. A Review of Challenges and Opportunities Associated with Bolted Flange Connections in the Offshore Wind Industry. Metals 2020, Vol 10, Page 732 [Internet]. 2020 Jun 1 [cited 2023 Mar 29];10(6):732. Available from: https://www.mdpi.com/2075-4701/10/6/732/htm
4. Lochan S, Mehmanparast A, Wintle J. A review of fatigue performance of bolted connections in offshore wind turbines. Procedia Structural Integrity. 2019 Jan 1;17:276–83.
5. Braithwaite J, Goenaga IG, Tafazzolimoghaddam B, Mehmanparast A. Sensitivity analysis of friction and creep deformation effects on preload relaxation in offshore wind turbine bolted connections. Applied Ocean Research. 2020 Aug 1;101:102225.
6. Wind energy in Europe 2021 Statistics and the outlook for 2022-2026. 2018;
7. Johnson KL. Contact Mechanics [Internet]. Cambridge University Press; 1985 [cited 2023 Mar 29]. Available from: https://www.cambridge.org/core/product/identifier/9781139171731/type/book
8. Li Y, Huang R, Zhao S, Wang J. Contact pressure analysis of pin-loaded lug with clearance. Research Article Advances in Mechanical Engineering [Internet]. [cited 2023 Mar 8];2022(6):1–15. Available from: https://us.sagepub.com/en-us/nam/open-access-at-sage
9. Siemens SWT-6.0-154 - 6,00 MW - Wind turbine [Internet]. [cited 2023 Mar 29]. Available from: https://en.wind-turbine-models.com/turbines/657-siemens-swt-6.0-154#datasheet
10. Offshore Wind Turbine SWT-6.0-154 I Siemens Gamesa [Internet]. [cited 2023 Mar 29]. Available from: https://www.siemensgamesa.com/products-and-services/offshore/wind-turbine-swt-6-0-154
11. Ryan H, Annoni A, Winkes J, Mehmanparast A. Optimising design parameters for offshore wind MP-TP wedge

connection technology using analytical techniques. Ocean Engineering. 2023 Jan 15;268:113562.
12. Igwemezie V, Mehmanparast A, Kolios A. Current trend in offshore wind energy sector and material requirements for fatigue resistance improvement in large wind turbine support structures – A review. Renewable and Sustainable Energy Reviews. 2019 Mar 1;101:181–96.
13. Creusen KEY, Misios G, Winkes JS, Veljkovic M. Introducing the C1 Wedge Connection. Steel Construction [Internet]. 2022 Feb 1 [cited 2023 Mar 15];15(1):13–25. Available from: https://onlinelibrary.wiley.com/doi/full/10.1002/stco.202100039
14. EN 1993-1-8: Eurocode 3: Design of steel structures - Part 1-8: Design of joints.